# Biological Gender Classification from fMRI via Hyperdimensional Computing

Ryan Billmeyer

Dept. Electrical & Computer Engineering

University of Minnesota

Minneapolis, MN USA

billm038@umn.edu

Keshab K. Parhi

Dept. Electrical & Computer Engineering

University of Minnesota

Minneapolis, MN USA

parhi@umn.edu

Abstract-Hyperdimensional (HD) computing is a braininspired form of computing based on the manipulation of highdimensional vectors. Offering robust data representation and relatively fast learning, HD computing is a promising candidate for energy-efficient classification of biological signals. This paper describes the application of HD computing-based machine learning to the classification of biological gender from restingstate and task functional magnetic resonance imaging (fMRI) from the publicly available Human Connectome Project (HCP). The developed HD algorithm derives predictive features through mean dynamic functional connectivity (dFC) analysis. Record encoding is employed to map features onto hyperdimensional space. Utilizing adaptive retraining techniques, the HD computing-based classifier achieves an average biological gender classification accuracy of 87%, as compared to 84% achieved by edge entropy measure.

#### I. Introduction

The prevalence of IoT (interenet of things) devices has led to the emergence of the distributed computing framework for edge computing. In edge computing, bandwidth intensive tasks are performed within an IoT device as opposed to sending data to the cloud for processing [1], leading to load reductions in cloud networks, decreases in response times, and the localization of user data. Edge computing is attractive for the resource intensive task of machine learning [2]. However, this approach is hampered by state-of-the-art machine learning algorithms being too computationally expensive to run on resource-limited IoT devices [3]. Thus, machine learning with edge computing necessitates the development of algorithms that balance efficiency with performance.

Hyperdimensional (HD) computing is a brain-inspired computing framework that has been shown to produce energy-efficient classifiers while retaining acceptable accuracy. HD computing differs from traditional computing methods in that it computes with high-dimensional ( $D \geq 1,000$ ) vectors. These hyperdimensional vectors are meant to mimic neural states within the human brain [4]. HD computing has been shown to be a viable alternative in a myriad of different classification tasks such as text categorization [5], speech recognition [6], DNA sequencing [7], and language recognition [8]. In particular, there have been many successful applications

This paper has been supported in part by the NSF under grant number CCF-1814759.

of HD computing-based classification to biological signals including EMG gesture detection [9], ECoG seizure detection [10], and EEG event-error detection [11]. While performing classification with these high-temporal resolution biological signals, HD computing has been shown to achieve high accuracy while using significantly less resources and training data than competing algorithms. However, there is no literature, to the best knowledge of the authors, on the effectiveness of HD computing in machine learning tasks centered on acquisition methods for biological signals with low-temporal resolution, such as functional magnetic resonance imaging (fMRI).

In neuroimaging, several applications have investigated the use of fMRI in predicting individual attributes (age [12], gender, fluid IQ, and fluid ability [13]) of a subject via machine learning. Traditionally, these models assume that functional connectivity within the brain is stationary over time, referred to as static functional connectivity [14]. However, it has been recently shown that analysis methods for dynamic functional connectivity (dFC) can be extended to fMRI [15]. Often used in high-temporal resolution biological signals, dynamic functional connectivity differs from its static counterpart in that it is able to capture spatio-temporal fluctuations in correlation between brain regions [16]. The use of dynamic functional connectivity in deriving features for classification has been reported to exceed or match the performance of previous static methods in the prediction of biological gender [13].

This paper aims to extend dFC-based feature extraction to HD computing through the task of biological gender prediction via fMRI. In doing so, this paper also demonstrates a novel application of HD computing to classification of low-temporal resolution biological signals. The HDC classifier proposed in this paper is able to achieve a gender classification accuracy of 87%. The remaining sections of the paper are organized as follows. In Section 2, we outline the theoretical framework behind a high-performance HD computing-based classifier that utilizes record encoding [17] and retraining [18]. In Section 3, we detail the fMRI dataset, dFC-based feature extraction method, and HD model specifications used in the proposed model. In Section 4, we provide experimental results followed by comparison to state-of-the-art methods in biological gender classification via fMRI [13]. Section 5 concludes the paper.

#### II. HYPERDIMENSIONAL COMPUTING

#### A. Basics

HD computing (HDC) at its core is the manipulation of high dimensional vectors, referred to as hypervectors. A hypervector v of dimension  $d \geq 1,000$  can be binary ( $v \in \{0,1\}^d$ ), bipolar ( $v \in \{-1,1\}^d$ ), or real-valued ( $v \in \mathbb{R}^d$ ). Real-valued hypervectors store significantly more information than their rudimentary counterparts at the expense of increased memory usage. As a result, binary hypervectors are often implemented in HDC models that prioritize efficiency over accuracy. However, techniques for training HDC models using higher fidelity real-valued hypervectors and then compressing through compHD [3] or binarization [19] have been proposed.

When working with hypervectors, there exist three standard operations: multiplication, addition, and permutation (MAP). Definitions of the MAP operations differ between the various types of hypervectors [20]. The proposed method in this paper utilizes multiplication as defined for binary hypervectors and addition as defined for real-valued hypervectors. In this sense, mulitplication is performed by evaluating the XOR of two binary hypervectors while addition is simply element-wise addition of n real-valued hypervectors.

## B. Record Encoding

In the same vein as feature scaling data for gradient descent-based algorithms in traditional machine learning, data transformations are required for HDC models to perform optimally. In the proposed method, a time-series consisting of n samples must be mapped onto a hypervector in d-dimensional space. Within HD computing, one of several processes used for creating robust representations of time-series data in hyperdimensional space is record encoding [17].

Record encoding consists of binding temporal locations of samples to their respective values via multiplication. To achieve this, each sample index is assigned a randomly generated representative hypervector. The collection of n orthogonal hypervectors, representing the n sample locations, are stored in item memory (IM). In a similar fashion, the range of values that a sample can take are quantized into bins represented by hypervectors stored in the continuous item memory (CiM). The minimum bin value of the signal is assigned to a randomly generated base hypervector. For mapping hypervectors to increasing bin values, a defined number of distinct bits are flipped each time such that the hypervector representing the maximum value bin approximately represents the negation of the base hypervector. The process of successive bit flipping preserves the locality of signal values in high dimensional space. The number of hypervectors present in the CiM is dependent upon the precision required. The implementation of an m-level CiM for an n sample signal is displayed in Fig. 1. Each sample location is bound to its value through the multiplication of the corresponding IM and CiM hypervectors. The n resulting hypervectors are summed to create a single encoded hypervector representative of the original data.

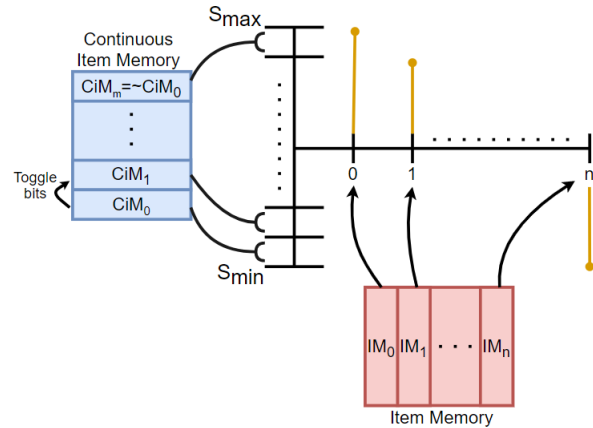


Fig. 1. HDC memory structure for record encoding [17]. CiM hypervectors are mapped onto value ranges. IM hypervectors are mapped to sample indices.

## C. Classification and Retraining

A useful property of hypervectors is that any two randomly generated hypervectors are orthogonal to each other with high probability [20]. This property implies that measures of orthogonality between hypervectors can double as measures of similarity. With real-valued hypervectors, the standard measurement of similarity is the cosine similarity given by:

$$Sim(A,B) = \frac{A \cdot B}{|A||B|} \tag{1}$$

Thus,  $Sim(A,B)\approx 0$  indicates orthogonal or dissimilar hypervectors while hypervectors with Sim(A,B) close to 1 are similar.

Similarity measurements form the basis of classification with HD computing. While passing over encoded training data, an HDC-based classifier sums all the training hypervectors in each class to construct a collection of class prototype hypervectors. Class prototype hypervectors, or simply class hypervectors, are representative of the typical hyperdimensional mapping of data belonging to a class. Classification of encoded query data is then accomplished through finding the closest class hypervector to the query hypervector via cosine similarity.

While HDC-based classification has been touted as capable of one-shot learning [11], the performance of an HDC model has been shown to significantly improve via the use of AdaptHD retraining [18]. Retraining in HDC-based classifiers is achieved through the alteration of a model's class hypervectors. The AdaptHD framework features two retraining methods: iteration dependent and data dependent. In both methods, the incorrect classification of an encoded training sample Q from the class corresponding to class hypervector  $C_{correct}$  is penalized according to the following scheme:

$$C_{correct} = C_{correct} + \alpha Q \tag{2}$$

$$C_{wrong} = C_{wrong} - \alpha Q \tag{3}$$

where  $C_{wrong}$  is the class hypervector of the incorrectly predicted class and  $\alpha$  is the learning rate. The value of  $\alpha$  in iteration dependent retraining is set after each epoch based

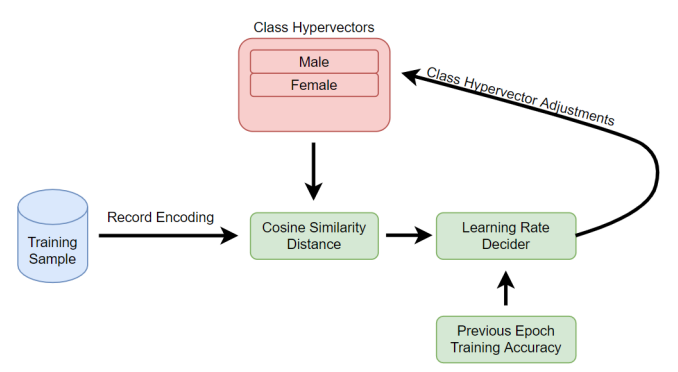


Fig. 2. AdaptHD [18] iteration and data dependent retraining. Incorrect classification of a training example is penalized by altering class hypervectors.

on the training accuracy of the model. Intuitively, a lower training accuracy corresponds to a larger  $\alpha$  value. In contrast, the learning rate in data dependent retraining is decided on an individual basis for each incorrectly classified training example. Specifically, the model performance within data dependent retraining is based on cosine similarity distance from the correct class,  $Sim(Q, C_{Wrong}) - Sim(Q, C_{Correct})$ , where a larger distance necessitates a greater  $\alpha$  value. In both cases, user-defined look-up tables map a cosine similarity distance or training accuracy to a respective  $\alpha$  value. In general, hyper-parameters within AdaptHD consist of the maximum value defined for  $\alpha$  and the number of retraining iterations performed. The two methods stated can be combined by tracking independent learning rates and then averaging when altering class hypervectors. A high level overview of AdaptHD retraining penalizing an incorrect prediction on training data is illustrated in Fig. 2.

## III. PROPOSED METHOD

### A. Dataset

The fMRI data used is sourced from the Q2 data release of the publicly available Human Connectome Project (HCP) Database. The HCP dataset consists of 477 subjects each with 8 distinct brain scans. The demographic spread of subjects within the dataset is as follows: 198 males, 297 females. As outlined in the HCP procedures, a subject has their brain imaged via fMRI while performing 1 of 7 different tasks or in resting state [21]. The latter is referred to as task fMRI while the former is resting-state fMRI. The seven tasks performed by subjects include: emotional processing, gambling, working memory, relational, language processing, motor function, and social processing. The raw fMRI data is processed following the procedure outlined in [13] to produce thousands of blood oxygen level dependent (BOLD) signals corresponding to fluctuations in blood flow between 2 mm isotropic voxels in the brain. To reduce the dimensionality of the data, 85 brain regions of interest are identified using the Freesurfer cortical parcellation atlas [22]. The mean BOLD signal of all the voxels in each of the 85 regions is then calculated, resulting in 85 BOLD time-series per task for each subject. The temporal resolution of the BOLD signals for each subject is 1Hz on average across task and resting state [21].

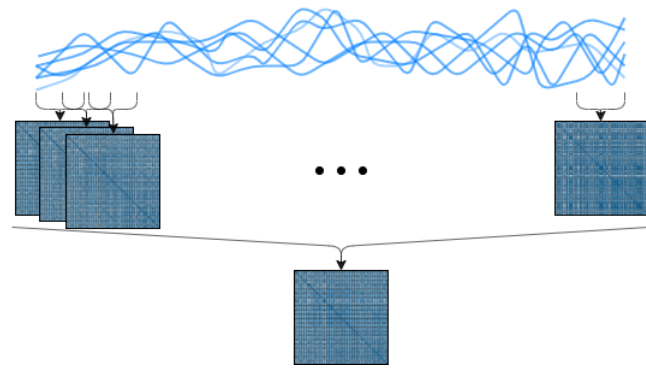


Fig. 3. Mean dFC. Absolute correlation coefficient matrices are calculated for each window and then averaged over the BOLD signal duration.

#### B. Feature Extraction via Mean dFC

For feature extraction, dynamic functional connectivity of the BOLD signals collected from the 85 regions of interest is calculated through the sliding window correlation method [23]. The BOLD signal is first multiplied by a sliding window function to isolate the pertinent samples. These samples are then used to calculate an  $85\times85$  matrix of absolute Pearson correlation coefficients. The sliding window is shifted forward by a set number of samples and the process is repeated for the duration of the signal. The length of sliding window used was 68 samples, corresponding to approximately 50s, as suggested in [24]. In addition, various levels of window stride length (5,10,15) were tested to determine an optimal value of 10 samples per shift, resulting in a 58 sample overlap between windows.

The set of correlation matrices that result from dFC analysis can be decomposed through several different methods. In previous works, ICA, PCA, and PARAFAC decomposition have all been applied to the windowed correlation matrices to extract 25 to 75 brain states that function as classification features. However, the proposed model opts for the computationally lean method of mean dFC [13]. In contrast to existing resource intensive decomposition methods, mean dFC simply takes the element-wise average of the set of absolute Pearson correlation matrices. The resulting mean dFC matrix is of dimension  $85 \times 85$  and contains  $\binom{85}{2} = 3570$  distinct classification features due to symmetry in the correlation matrices. The process of calculating mean dFC is illustrated in Fig. 3. Note that mean dFC results in a high dimensional feature space; however, HD computing has been shown to not require domain expert knowledge for feature selection [11]. Thus, no feature selection is performed by the model proposed in this work.

## C. Limitations

There are several data limitations present when using fMRI data sourced from the HCP database. Most notably, task fMRI scans and resting-state fMRI scans have transient durations of 3-6 minutes and 12 minutes, respectively. Given the low temporal resolution of the signals, learning with each of the scan types by themselves can lead to a model with poor predictive abilities. To extend signal duration, the BOLD

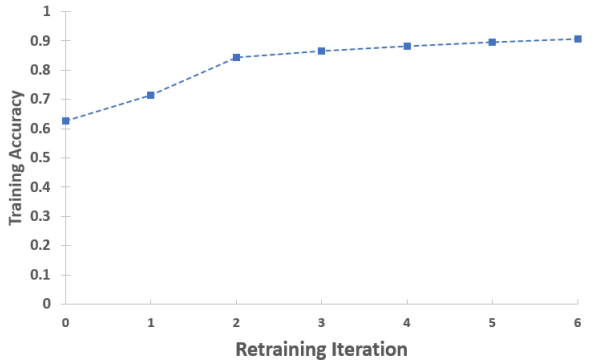


Fig. 4. Training accuracy of HDC biological gender classifier through successive iterations of retraining.

signals from each task and the resting-state are concatenated to create a single combined fMRI scan. This requires that all 8 fMRI scans are present for a subject, which is valid for 477 subjects in the Q2 release. To further compensate for data limitations, additional training data is generated via sliding window [25]. Through this technique, the number of training samples is increased by a factor of 84.

## D. Proposed HDC Classifier

The proposed HDC-based classifier prioritizes high performance gender classification over all else. To that end, real-valued hypervectors with d=10,000 are used along with both iteration and data dependent retraining. Mean dFC feature extraction is carried out on combined BOLD signal data to create an  $85\times85$  mean dFC matrix for each training sample. All distinct feature values of the mean dFC matrix are contained in either the lower or upper triangle of the matrix. Thus, the lower triangle of a mean dFC matrix is flattened and mapped onto a hypervector via record encoding. An initial pass over the training data is performed such that the model trains two preliminary class hypervectors. Both retraining methods are then used to enforce high training accuracy.

## IV. EXPERIMENTAL RESULTS

The proposed HDC-based classifier is validated through 5-fold cross-validation (CV) [26]. The 477 subjects are distributed evenly into five folds, four of which are used for training the model while the remaining fold serves as test data. Using in-fold validation, the optimal number of retraining steps in AdaptHD was determined as six. The maximum  $\alpha$  values were 0.3 and 1.2 for iteration and data dependent retraining, respectively. Fig. 4 demonstrates the significant improvements in model training accuracy achieved through retraining. For characterization of the HDC model's performance, the standard classification metrics of accuracy, sensitivity (female accuracy), and specificity (male accuracy) are reported. All reported results are averaged over ten executions of the model to account for variations in testing accuracy.

The total gender classification accuracy of the proposed HDC model across all available types of fMRI data is reported in Fig 5. The HDC-based classifier is able to maintain a classification accuracy above 70% in all forms of fMRI task

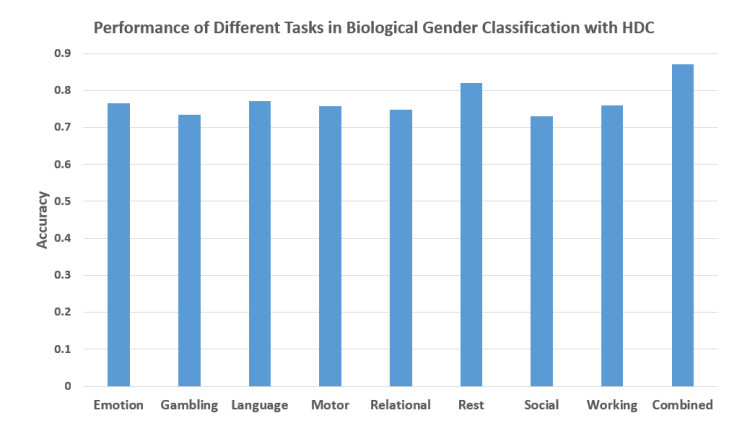


Fig. 5. Performance of proposed HDC biological gender classifier across the various categories of fMRI data.

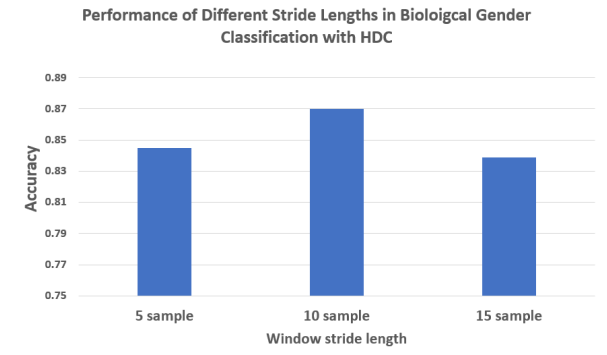


Fig. 6. Performance of proposed HDC biological gender classifier across various dFC sliding window stride lengths.

data. Resting-state fMRI data leads to the highest accuracy of all the uncombined data types at 82%. The concatenation of all 8 forms of fMRI data into a single combined time-series leads to a classification accuracy of 87%. As discussed in Section 3, the comparatively longer BOLD signals in rest and combined fMRI data most likely lend to the increases in classification accuracy achieved through using these scan types. In terms of feature extraction methods, the performance of the HDC classifier with several mean dFC sliding window stride lengths is shown in Fig. 6. As indicated in Section 3, a stride length of 10 samples is optimal; however, high accuracy results are achieved with all three options.

The performance of the HDC classifier with combined fMRI data type is compared against existing state-of-the-art biological gender classification via fMRI methods in Table I. All methods stated in Table I were executed using the Q2 release of the HCP and 5 fold CV. The state-of-the-art methods presented utilize the widely popular and powerful random forest machine learning algorithm. The proposed HDC-based classifier is able to achieve 87% total accuracy with 92% sensitivity and 80% specificity, surpassing the overall performance of 8 out of the 9 reported methods. In addition, the proposed model and constrained PARAFAC decomposition with random forest are the only two methods able to surpass 90% female classification accuracy while retaining at least 80% male classification accuracy. The highest performing feature extraction

TABLE I
COMPARISON OF RESULTS FOR BIOLOGICAL GENDER
CLASSIFICATION VIA FMRI [13]

Method	Features	Accuracy	Sensitivity	Specificity
Constrained PARAFAC	25	0.94	0.97	0.87
HDC Mean dFC (proposed)	3570	0.87	0.92	0.80
Edge Entropy	3570	0.84	0.89	0.81
Partial Least Squares	15	0.80	0.66	0.86
Node Entropy	85	0.75	0.83	0.66
Random Forest Mean dFC	3570	0.74	0.85	0.66
Correlation	15	0.73	0.64	0.75
dFC ICA	75	0.71	0.55	0.85
Network Features	54	0.69	0.74	0.65
dFC PCA	75	0.5	0.48	0.51

method of constrained PARAFAC decomposition was tested with the proposed HDC-based classifier but led to negative results. It may be noted that the PARAFAC method requires tensor decomposition and is computationally more complex.

We note that the mean dFC feature extraction method saw a 13% increase in overall performance when utilized in the proposed HDC model as opposed to the random forest algorithm. Using this lean feature extraction method, HDC serves as a higher performance alternative to the traditional random forest algorithm. Finally, the proposed model outperforms both methods, edge entropy and mean dFC with random forest, that retained a 3570 dimension feature space, indicating that HDC-based classification has a higher tolerance for noise in the extracted features.

#### V. CONCLUSION

In this paper, we have demonstrated how classification with hyperdimensional computing can be extended to the task of biological gender detection via fMRI. The proposed HDC-based classifier employs the AdaptHD retraining framework and mean dFC feature extraction. Through these methods, the proposed HDC biological gender model is able to achieve an overall performance of 87% accuracy with 92% accuracy for females and 80% accuracy for males. This performance was shown to be at par with leading methods of biological gender classification via fMRI. Future work will address the extension of mean dFC feature extraction to seizure detection via HD computing. The applications of HD computing-based classification to predicting fluid intelligence and fluid ability via fMRI will also be investigated using the framework presented in this paper.

#### REFERENCES

- W. Shi, J. Cao, Q. Zhang, Y. Li, and L. Xu, "Edge computing: Vision and challenges," *IEEE Internet of Things Journal*, vol. 3, no. 5, pp. 637–646, 2016.
- [2] D. Xu et al., "Edge intelligence: Architectures, challenges, and applications," in arXiv:2003.12172, 2020. https://arxiv.org/abs/2003.12172.
- [3] J. Morris, M. Imani, S. Bosch, A. Thomas, H. Shu, and T. Rosing, "Comphd: Efficient hyperdimensional computing using model compression," in 2019 IEEE/ACM International Symposium on Low Power Electronics and Design (ISLPED), pp. 1–6, 2019.
- [4] P. Kanerva, "Hyperdimensional computing: An introduction to computing in distributed representation with high-dimensional random vectors," *Cognitive Computation*, vol. 1, pp. 139–159, 2009.

- [5] F. R. Najafabadi, A. Rahimi, P. Kanerva, and J. Rabaey, "Hyperdimensional computing for text classification," in *Design, Automation Test in Europe Conference Exhibition (DATE), University Booth*, pp. 1–1, 2016.
- [6] M. Imani, D. Kong, A. Rahimi, and T. Rosing, "Voicehd: Hyperdimensional computing for efficient speech recognition," in 2017 IEEE International Conference on Rebooting Computing (ICRC), pp. 1–8, 2017.
- [7] M. Imani, T. Nassar, A. Rahimi, and T. Rosing, "Hdna: Energy-efficient dna sequencing using hyperdimensional computing," *IEEE International Conference on Biomedical and Health Informatics 2018*.
- [8] A. Rahimi, P. Kanerva, and J. M. Rabaey, "A robust and energy-efficient classifier using brain-inspired hyperdimensional computing," in *Proceed*ings of the 2016 International Symposium on Low Power Electronics and Design, p. 64–69, Association for Computing Machinery, 2016.
- [9] A. Rahimi, S. Benatti, P. Kanerva, L. Benini, and J. M. Rabaey, "Hyperdimensional biosignal processing: A case study for emg-based hand gesture recognition," in 2016 IEEE International Conference on Rebooting Computing (ICRC), pp. 1–8, 2016.
- [10] A. Burrello, K. Schindler, L. Benini, and A. Rahimi, "One-shot learning for ieeg seizure detection using end-to-end binary operations: Local binary patterns with hyperdimensional computing," in 2018 IEEE Biomedical Circuits and Systems Conference (BioCAS), pp. 1–4, 2018.
- [11] A. Rahimi, P. Kanerva, J. del R. Millân, and J. M. Rabaey, "Hyperdimensional computing for noninvasive brain-computer interfaces: Blind and one-shot classification of eeg error-related potentials," EAI, 3 2017.
- [12] R. M. Hutchison and J. B. Morton, "Tracking the brain's functional coupling dynamics over development," *Journal of Neuroscience*, vol. 35, no. 17, pp. 6849–6859, 2015.
- [13] B. Sen and K. K. Parhi, "Predicting biological gender and intelligence from fmri via dynamic functional connectivity," *IEEE Transactions on Biomedical Engineering*, vol. 68, no. 3, pp. 815–825, 2021.
- [14] S. Menon and K. Krishnamurthy, "A comparison of static and dynamic functional connectivities for identifying subjects and biological sex using intrinsic individual brain connectivity," *Scientific Reports*, vol. 9, 04 2019.
- [15] C. Chang and G. Glover, "Time-frequency dynamics of resting-state brain connectivity measured with fmri," *NeuroImage*, vol. 50, pp. 81– 98, 03 2010.
- [16] M. G. Preti, T. A. Bolton, and D. Van De Ville, "The dynamic functional connectome: State-of-the-art and perspectives," *NeuroImage*, vol. 160, pp. 41–54, 2017. Functional Architecture of the Brain.
- [17] A. Rahimi, S. Benatti, P. Kanerva, L. Benini, and J. M. Rabaey, "Hyperdimensional biosignal processing: A case study for emg-based hand gesture recognition," in 2016 IEEE International Conference on Rebooting Computing (ICRC), pp. 1–8, 2016.
- [18] M. Imani, J. Morris, S. Bosch, H. Shu, G. D. Micheli, and T. Rosing, "Adapthd: Adaptive efficient training for brain-inspired hyperdimensional computing," in 2019 IEEE Biomedical Circuits and Systems Conference (BioCAS), pp. 1–4, 2019.
- [19] M. Imani, J. Messerly, F. Wu, W. Pi, and T. Rosing, "A binary learning framework for hyperdimensional computing," in 2019 Design, Automation Test in Europe Conference Exhibition (DATE), pp. 126–131, 2019
- [20] L. Ge and K. K. Parhi, "Classification using hyperdimensional computing: A review," *IEEE Circuits and Systems Magazine*, vol. 20, no. 2, pp. 30–47, 2020.
- [21] D. C. Van Essen et al., "The wu-minn human connectome project: An overview," NeuroImage, vol. 80, pp. 62–79, 2013. Mapping the Connectome.
- [22] R. S. Desikan et al., "An automated labeling system for subdividing the human cerebral cortex on mri scans into gyral based regions of interest," *NeuroImage*, vol. 31, no. 3, pp. 968–980, 2006.
- [23] A. Savva, G. Mitsis, and G. Matsopoulos, "Assessment of dynamic functional connectivity in resting-state fmri using the sliding window technique," *Brain and Behavior*, 03 2019.
- [24] N. Leonardi and D. Van De Ville, "On spurious and real fluctuations of dynamic functional connectivity during rest," *NeuroImage*, vol. 104, p. 430—436, January 2015.
- [25] I. Ullah, M. Hussain, E. ul Haq Qazi, and H. Aboalsamh, "An automated system for epilepsy detection using eeg brain signals based on deep learning approach," *Expert Systems with Applications*, vol. 107, pp. 61– 71, 2018.
- [26] S. Arlot and A. Celisse, "A survey of cross-validation procedures for model selection," *Statistics Surveys*, vol. 4, no. none, pp. 40 – 79, 2010.